Molecular Dynamics Investigation of Membrane-Bound Bundles of the Channel-Forming Transmembrane Domain of Viral Protein U from the Human Immunodeficiency Virus HIV-1

Carlos F. Lopez,† Mauricio Montal,* J. Kent Blasie,† Michael L. Klein,† and Preston B. Moore†
*Division of Biology, University of California, La Jolla, California 92093-0346; and †Department of Chemistry, University of Pennsylvania, Philadelphia, Pennsylvania 19104-6323 USA

ABSTRACT Molecular dynamics (MD) simulations have been carried out on bundles of the channel-forming transmembrane (TM) domain of the viral protein U (VPU^{1-27} and VPU^{6-27}) from the human immunodeficiency virus (HIV-1). Simulations of hexameric and pentameric bundles of VPU^{6-27} in an octane/water membrane mimetic system suggested that the pentamer is the preferred oligomer. Accordingly, an unconstrained pentameric helix bundle of VPU^{1-27} was then placed in a hydrated palmitoyl-oleyl-3-*n*-glycero-phosphatidylethanolamine (POPE) lipid bilayer and its structural properties calculated from a 3-ns MD run. Some water molecules, initially inside the channel lumen, were expelled halfway through the simulation and the bundle adopted a conical structure reminiscent of previous MD results obtained for VPU^{6-27} in an octane/water system. The pore constriction generated may correspond to a closed state of the channel and underlies the relocation of the W residue toward the pore lumen. The relative positions of the helices with respect to the bilayer and their interactions with the lipids are discussed. The observed structure is stabilized via specific interactions between the VPU helices and the carbonyl oxygen atoms of the lipid molecules, particularly at the Q and S residues.

INTRODUCTION

Viral protein U (VPU) is an accessory protein present in all strains of the human immunodeficiency virus 1 (HIV-1). Depending on the HIV variant, VPU has 80–82 residues and is composed of two distinct domains (Frankel and Young, 1998; Turner and Summers, 1999). The first domain involves a transmembrane (TM) portion of the protein (roughly residues 1–30) that has been linked to the enhancement of virion release from the host cell (Schubert *et al.*, 1996a). The second domain is cytoplasmic (residues 31–80, 82), and has been associated with the degradation of CD4 in the host cell surface (Schubert *et al.*, 1996b; Tiganos *et al.*, 1998; Lamb and Pinto, 1997). Structural NMR studies of VPU in solution, using expressed monomers of different sizes, have shown that VPU contains three α-helical subunits (Marassi *et al.*, 1999; Zheng *et al.*, 2001). One of these, composed roughly of residues 1–28, corresponds to the TM domain (VPU-TM), while the remainder of the peptides correspond to experimentally observed α-helices in the cytoplasmic domain. VPU-TM has been shown to form ion channels that are selective to monovalent cations, in particular Na^+ and K^+ (Schubert *et al.*, 1996b). It has been suggested that the ion channel is formed by the homooligomeric aggregation of four to seven proteins (Willbold *et al.*, 1997). Previous workers argued that the most probable oligomeric state is a pentamer based upon combinations of modeling and experiment (Grice *et al.*, 1997; Kukol and Arkin, 1999). However, recent studies suggest that there is more than one possible state of the channel and the exact oligomeric state of the helix bundle is therefore not known with certainty.

Solid-state NMR and x-ray reflectivity studies show that the amphipathic helices in the cytoplasmic domain of VPU lie approximately parallel to and on the surface of the membrane, while the TM domain, which is mostly hydrophobic, lies approximately normal to the bilayer surface (Marassi *et al.*, 1999; Zheng *et al.*, 2001). The orientation of these domains has been confirmed for VPU and other ion channels by using NMR to probe the tilt angle (Zheng *et al.*, 2001; Marassi and Opella, 2000). Computational approaches to the elucidation of the structure of TM proteins have also shown that small proteins topologically similar to VPU will align more or less perpendicular to the bilayer surface (Sansom *et al.*, 1998).

We present here the results of two separate MD simulations of bundles of VPU-TM segments: 1) a hexamer of VPU^{6-27} in octane/water bilayer mimetic and 2) a pentamer of VPU^{1-27} in a hydrated lipid bilayer. The simulation of a VPU^{6-27} hexamer in an octane/water slab follows the same procedure as in our previous work on the pentamer and uses the same peptide (VPU^{6-27}) in an attempt to establish the preferred oligomeric state (Moore *et al.*, 1998). Anticipating our results, we find that the hexamer expels a VPU^{6-27} monomer, thus generating a pentameric bundle. We then proceed to a more detailed MD study of an all-atom model of a pentameric VPU^{1-27} bundle in an explicit, fully hydrated POPE lipid bilayer.

Submitted October 16, 2001, and accepted for publication January 16, 2002.

Address reprint requests to Michael L. Klein, 231 S. 34th St., Philadelphia, PA 19104-6323. Tel.: 215-898-8571; Fax: 215-898-8296; E-mail: klein@lrsm.upenn.edu.

0006-3495/02/09/1259/09 $2.00

METHODS

General setup

The MD calculations utilize our in-house Center for Molecular Modeling Molecular Dynamics (CM^3D) program, which allows the simulation of a

wide variety of ensembles, ranging from constant energy (NVE) to fully flexible constant pressure and constant temperature (NPT) (Moore and Klein, 1997). The simulation methodology used in the present work is very similar to that used previously by our group, and we therefore provide only a brief description of the methods in the present section and refer the interested reader to previous literature (Moore *et al.,* 2001). The simulations used the following sequences: I^{6}AIVALVVAIIIAIVVWSIVII^{27} for VPU$^{6-27}$ and M^{1}EPIQIAIVALVVAIIIAIVVWSIVII^{27} for VPU$^{1-27}$ (letter and number of residues used throughout the text). The latter has been shown to exhibit ion channel activity in conductance experiments (Schubert *et al.,* 1996b).

The RESPA multiple time step integrator scheme, which allows the use of a much longer time step than would normally be required to integrate the evolution of the faster motions, enabled us to improve the wall clock efficiency of the code (Tuckerman *et al.* 1992; Tuckerman and Martyna, 2000). Periodic boundary conditions in three dimensions were also used in this simulation, and the short-range van der Waals interactions were truncated at 10 Å. Given the importance of electrostatic interactions, we do not truncate but rather treat the full electrostatics interactions via Ewald sums (Feller *et al.,* 1996; Norberg and Nelsson, 2000). The simulation was run on a multi-processor parallel platform with the replicated data technique (Moore and Klein, 1997).

For the hexamer study we use the same procedures as in a previous paper, where a pentamer was inserted in an octane/water slab (Moore *et al.,* 1998). Briefly, the MD simulation was run at 300 K with the CHARMM19 force fields for VPU$^{6-27}$ (Brooks *et al.,* 1983). The octane layer used to mimic the hydrocarbon part of a lipid bilayer was modeled using the parameter set recommended by Siepmann *et al.,* (1993), and the water was modeled using the TIP3P (Jorgensen *et al.,* 1983) potential. The system was equilibrated within an orthorhombic cell with flexible sides (constrained angles) in the constant pressure ensemble (NPT). The data collection phase was run in the constant volume, temperature (NVT) ensemble at a temperature of 300 K. The bilayer mimetic (united atom octane) was chosen for computational efficiency. Although this combination of models may not be accurate enough to reproduce the detailed information required to understand specific lipid bilayer interactions, it is likely sufficient to obtain qualitative structural information on the relative stability of various oligomers. This simulation contained 6 VPU$^{6-27}$ helices, 305 octane molecules, and 1625 water molecules.

The hexameric bundle of VPU$^{6-27}$-TM in the octane/water system was constructed by arranging the centers of mass of six VPU$^{6-27}$ in a hexagon array with edges of 10 Å. The bundle was then annealed in vacuum to eliminate nonphysical contacts between residues. The interior of the bundle was then solvated by inserting an equilibrated cylinder of water into the pore and removing water molecules within 2 Å of an O or H atom in the bundle. The bundle, including the pore water, was then inserted into a 30-Å-thick slab of octane, and a slab of water 25 Å thick was placed on the system. Solvating molecules were eliminated if any molecule was found within 2 Å of any other atoms. The dimensions of the initial simulation cell were $45 \times 45 \times 65$ Å, which gives an overall density (0.9 g/cc) similar to physiological conditions.

Initial conditions

The VPU$^{1-27}$ bundle/lipid system was constructed in three steps: first, the assembly and equilibration of a hydrated lipid bilayer; second, the creation of a cavity through the bilayer to accommodate the VPU$^{1-27}$ bundle; and third, insertion of the bundle and further equilibration before running dynamics. While nontrivial, the first step has been discussed extensively in previous papers and we therefore focus only on the second and third steps, and refer the reader to the References for details and discussion (Moore *et al.,* 2001).

For the VPU$^{1-27}$ pentamer simulation in POPE we have used a similar setup to that published previously (Moore *et al.,* 2001). The CHARMM27

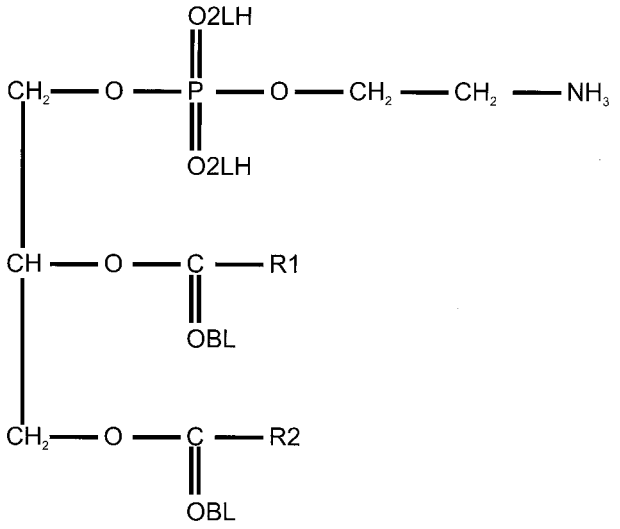

FIGURE 1 Schematic representation of the atoms surrounding the glycerol moiety in POPE.

force field, which has been shown to provide a good description of lipids and amino acids, was used (Feller *et al.,* 1997; Mackerell *et al.,* 1998). The present simulation was carried out using the NPT ensemble for both the equilibration and data collection. For the initial equilibration of the POPE bilayer without VPU$^{1-27}$, which consisted of 64 lipids and 2000 water molecules, we followed procedures reported previously (Moore *et al.,* 2001). Our choice of temperature corresponds to the liquid crystalline L_{α} phase with proper hydration (31 waters/lipid). Throughout the paper we refer to Fig. 1 for the naming of the atoms surrounding the glycerol moiety of the lipid molecule. Note that results obtained using the CHARMM19 force field were not transferred to the simulation using the CHARMM27 force field. Both simulations were started from scratch and are separate, except for the useful oligomeric information obtained from the VPU$^{6-27}$ simulation as discussed above.

To introduce the VPU$^{1-27}$ bundle into the bilayer it was necessary to make a hole in the membrane. After constructing an equilibrated and hydrated POPE bilayer we proceeded to the second step by inserting a membrane-spanning string of noninteracting, equidistant Lennard-Jones (LJ) particles normal to the bilayer surface (along the *z*-axis). To make this hole we inserted a rod-like chain of noninteracting van der Waals spheres that span the bilayer. The diameters of the spheres were increased slowly to minimize the disruption of the lipids. These LJ particles effectively make a cylinder having only van der Waals interactions. The diameter of the LJ particles is initially set to a small value (1 Å) and ~100 ps of dynamics is run. The size of the noninteracting particles is then increased and the dynamics are restarted until a large enough cavity (radius of ~14 Å) is obtained to accommodate the pentameric bundle along with channel-forming water molecules in the center of the pore. The lipid is then allowed to relax and accommodate the VPU$^{1-27}$-TM bundle. The whole system at the end of the equilibration phase was composed of 5 VPU$^{1-27}$ helices in a bundle, 64 POPE molecules, and 2085 water molecules. We find this method for opening a cavity through the bilayer by slowly growing a pore to be more robust and functional than removing lipid molecules because the lipid adjusts in a more natural fashion to the growing cavity rather than experiencing the removal of entangled lipids that contribute to the membrane structure. In addition, we find that equilibration around the helix bundle is faster with this approach because no major diffusion and readjustment needs to occur by the lipid molecules. These steps are not necessary in the octane/water case, as the octane readily adapts to the presence of the peptide bundle.

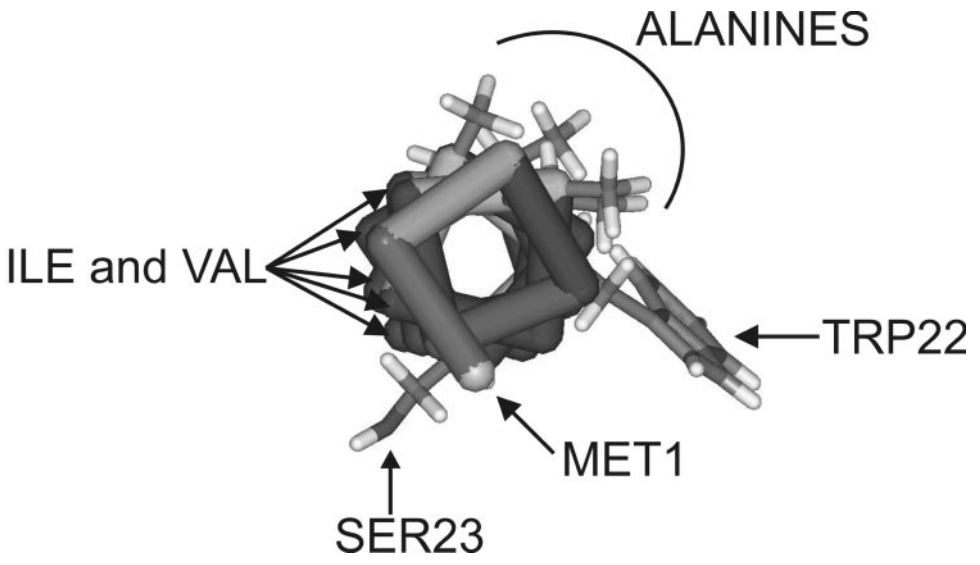

FIGURE 2 Stick view of the α carbon backbone of a VPU-TM monomer along the α-helix from the M(1) residue. The Ser and Trp groups are shown to illustrate their relative position to the Ala, Ile, and Val. Polar groups are represented in light gray, while nonpolar groups are represented in dark gray. Only the selected amino acids are shown explicitly for clarity.

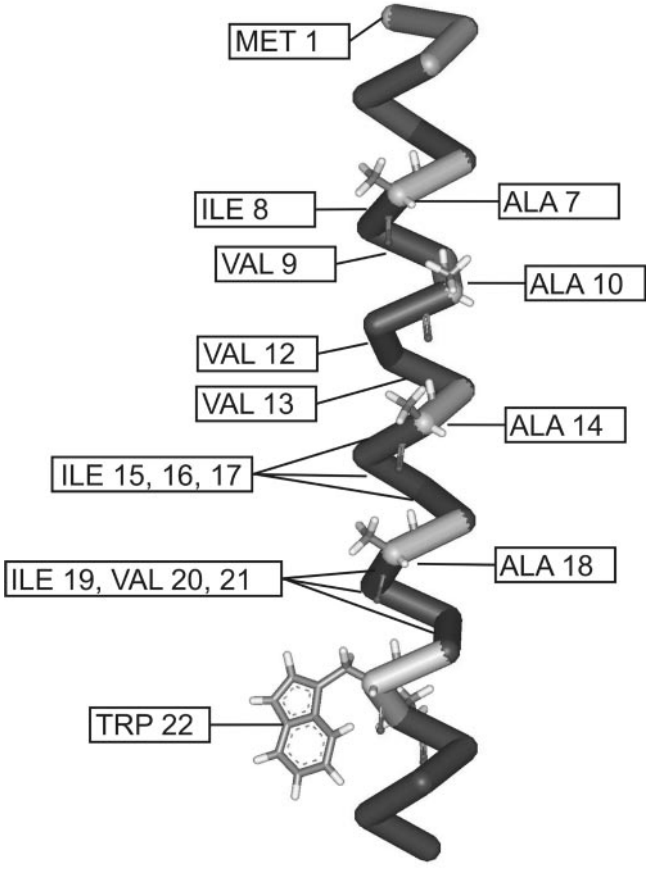

FIGURE 3 Stick view of the α carbon backbone of a VPU-TM monomer. The Ser, Ala, Trp, Ile, and Val groups are shown to illustrate their relative position along the length of the monomer. Polar groups are represented in light gray, while nonpolar groups are represented in dark gray. Only the smaller groups are shown explicitly for clarity.

Figs. 2 and 3 show an idealized α-helix structure of the VPU^{1-27} peptide monomer. Fig. 2 illustrates how the A residues are all on one-half of the cylindrical peptide, while the polar S is positioned on the opposite face along with mostly I and V residues, which are much more hydrophobic than A. Fig. 3 shows an alternative view of the monomer. Fig. 4 gives the initial structure of the pentamer based on results from the octane/water simulation (explained below). The VPU^{1-27} pentamer setup has the A residues facing toward the lumen of the pore because these groups are less hydrophobic than the alternative I and V that abound on the other face of the helix. This choice leaves the S residue facing toward the lipid bilayer. This setup is in agreement with experimental measurements by Arkin and co-workers, but differs from the choice made by Sansom *et al.*, (Kukol and Arkin, 1999; Sansom *et al.*, 1998). Once the peptide bundle was inserted into the bilayer, as shown in Fig. 4, it was constrained and water was inserted into the pore in the same fashion as with the VPU^{6-27} bundle in octane/water. Upon insertion, the VPU^{1-27} bundle and channel water were held fixed for 100 ps while the lipids were allowed to relax. All constraints were subsequently removed and the whole system was run with no constraints for another 500 ps. The data collection step was carried out subsequently with a total simulation time of 3 ns using a 1-fs time step.

The present simulation has been run at the Pittsburgh Supercomputing Center (PSC) on 32 nodes of the Cray T3E, 16 Nodes of an SGI origin 2000 at NCSA, and on local machines. The total simulation time resulted in ~60,000 CPU hours of single processor computer time.

STRUCTURE

In this section we examine some of the structural information obtained in the MD simulations. We first investigate the peptide bundle in the octane/water system and calculate detailed structural information of the hydrated VPU/POPE system. We report the electron density along the bilayer normal and radial distribution functions of different atom pairs to better understand the structural properties and specific interactions of the VPU^{1-27} bundle with the lipid.

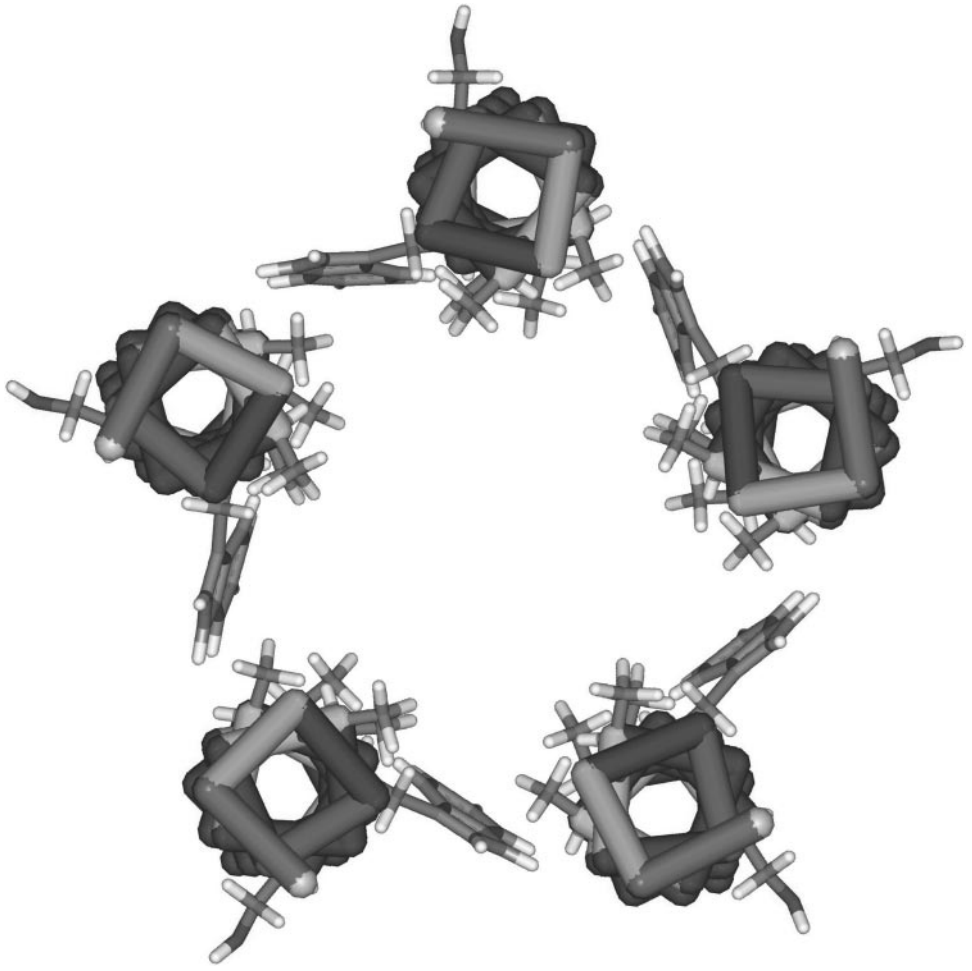

FIGURE 4 View of the initial idealized configuration of the pentamer before insertion into the bilayer. Polar residues are represented in light gray, while nonpolar residues are represented in dark gray.

VPU-TM as a hexamer in an octane/water mimetic bilayer

To gain a qualitative understanding of the structure and stability of the pentamer, and to address concerns that the oligomeric state could be a hexamer, we proceeded to run a hexameric VPU^{6-27}-TM in an octane/water system as described previously. Although we cannot obtain fine detail from this simulation we can see from Fig. 5 that under these conditions the preferred oligomeric state is that of a pentamer, and not a hexamer. The resulting pentameric structure agrees with previous simulations (Moore *et al.*, 1998). We have explored several simulations with different initial rotations along the long axis of the helix. This produced only minor variations in the resulting structures with a common motif of one expelled helix. The final positions of the W residues, which are somewhat indicative of the amount of rotation in the helices, vary with the choice of initial conditions but in general sit between helices, as seen previously (Kukol and Arkin, 1999). We thus conclude that under our simulation conditions the pentameric bundle is likely more stable than the hexamer and probably the preferred oligomeric state of VPU-TM. We do not observe any indication of shearing along the long axis for the α-helices.

VPU-TM as a pentamer in a hydrated POPE bilayer

With the knowledge gained from the octane/water simulations we turn our attention to the lipid system. After the various equilibration procedures described previously, the simulation was run for 3 ns. The initial structure remained in the open state for ~1 ns of simulation time, after which the first narrowing of the pore at the W was observed. This narrowing was further promoted by the exclusion of water molecules and their subsequent replacement by hydrophobic interactions between the V and I residues that lie below the W residue. Once these interactions began water was excluded from the W residues. This exclusion extended to the end of the C-terminus. The initial number of pore waters in the simulation varied between 64 and 67 during the first 500 ps, which diminished within the next 500 ps to ~45–50 water molecules. This reduction in water molecules in the

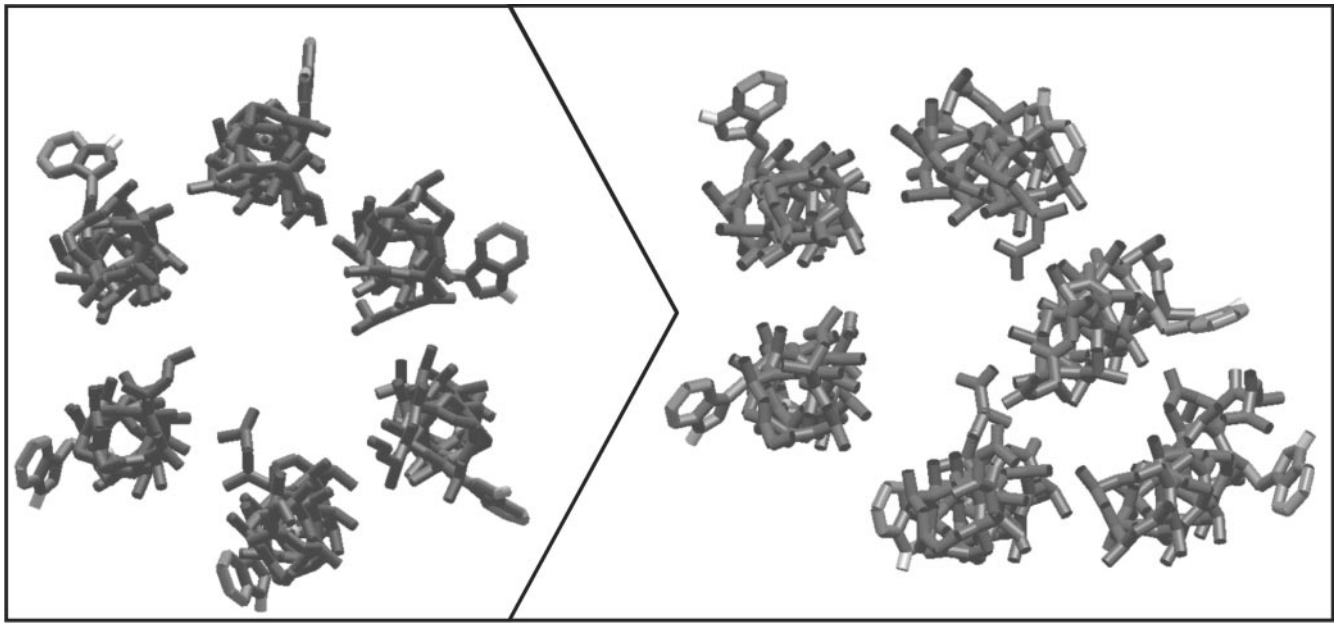

FIGURE 5 N-terminus view of the VPU-TM hexamer in membrane-mimetic octane/water. Starting configuration (*left*) and ending configuration (*right*) after 1 ns. The pentamer conformation seems favored in the present simulation conditions.

pore coincides with the narrowing of the pore near the W residue. In the remainder of the MD run the number of water molecules in the pore was constant at ~50. The evolution of the VPU^{1-27} pore is seen in three snapshots in Fig. 6, representing the initial configuration, a configuration halfway through the simulation, and a configuration at the end, respectively. After the first 1.5 ns the narrowing of the pore causes a funnel to be formed (Fig. 6, *center*). The final 1.5 ps of the simulation run exhibit a channel in a "closed" conformation state with a narrowing at the C-terminus of the pore (Fig. 6, *right*).

The quantities reported below were all averaged over the 3-ns data collection time of the simulation. In general, the average quantities were in good agreement with the octane/water and experimental results. The average length of the channel, measured as the distance between the centers of mass of residues 1 and 27, was found to be 43 Å. This value agrees with previous experimental and theoretical results

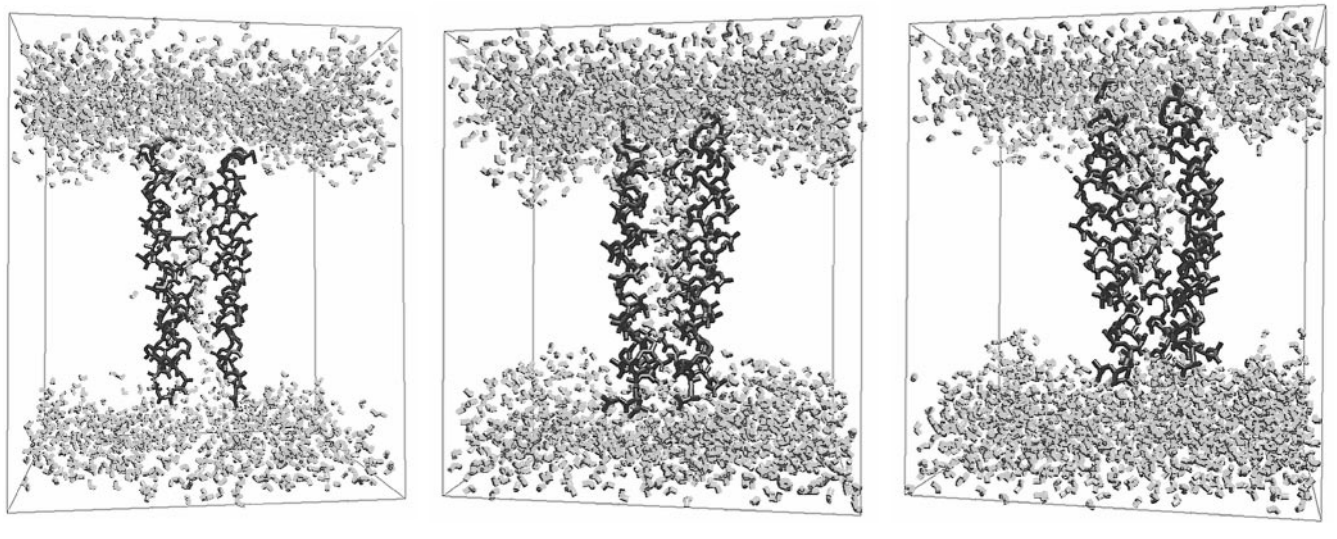

FIGURE 6 Snapshots of the evolution of the MD simulation at the beginning of the run (*left*), after 1.5 ns of MD (*center*), and at the end of the run (*right*). Water (*light gray*) is excluded from the lower part of the VPU-TM bundle (*dark gray*) at the end of the run, corresponding to a closed state of the VPU-TM bundle. The N-terminus of the pore is on the top and the C-terminus is on the bottom.

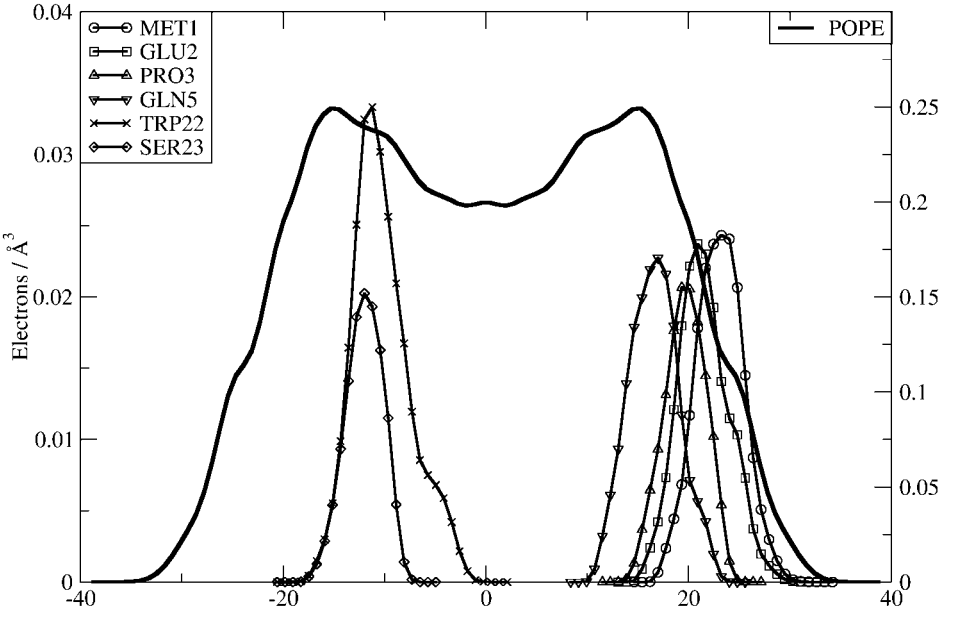

FIGURE 7 Electron density profile along the *z*-axis of the POPE lipid bilayer (*solid line*) and for Met (M), Glu (E), Pro (P), Gln (Q), Trp (W), and Ser (S) residues, thought to interact with the headgroups and water. Notice the difference in the electron density (*y*-axis) scale for POPE (*left*) and VPU residues (*right*).

and with typical bilayer spacing (Marassi *et al.*, 1999; Moore *et al.*, 1998; Gennis, 1989). The average tilt of the VPU$^{1-27}$ bundle was defined as the angle between the smallest component of the moment of inertia tensor and the bilayer normal. The resulting value of 6.3 ± 0.8° agrees well with data from Arkin and co-workers of 6.5 ± 1.7°, and is also in fair agreement with the previously reported value of 4.2° obtained from a simulation of a VPU$^{6-27}$ bundle in an octane/water system (Moore *et al.*, 1998; Kukol and Arkin, 1999).

To further understand how the pentameric bundle aligns inside the bilayer we plot the electron density profile of POPE and the electron densities of some important residues in Fig. 7. Although we have looked at all the interactions, we only report the electron density profiles along the *z*-axis for M, E, P, Q, W, and S to have an idea of the overall relative position of the ion channel. These residues were chosen because they exhibit the most overlap with the lipid headgroup. The M, E, and P residues are all shown above or slightly above the highest peak of the lipid bilayer electron density, corresponding to the phosphate group, which indicates that these groups are overlapping with the water and lipid headgroups. The M residue is the outermost residue in the N-terminus side and resides at the lipid/water interface. The Q residue, which was found to interact with the lipid carboxyl oxygen atoms, appears to lie slightly below the lipid headgroups at the hydrophobic/hydrophilic interface. This indicates that on average the preferential position of this residue is at about the carboxyl oxygen level, which is consistent with the radial distribution functions (RDFs) discussed below.

On the other side of the lipid bilayer, the S residue is positioned at the interface between the hydrophilic and hydrophobic residues. We find that S has a direct interaction with the carbonyl oxygen near the tails of the lipid. The bulky W residue sits slightly above the S residue and exhibits a relative position at the carboxyl oxygen level as well. However, no specific interaction between W and the carboxyl oxygen was found in our simulations. The C-terminus residue sits a little above the peak of the density corresponding to the phosphate groups, again suggesting that the C-terminus is accessible to the bulk water and the ethanolamine part of the headgroup.

All of the present MD simulations we have performed to date have resulted in a conical-shaped pore. As seen in Fig. 8, the pore size, calculated as the largest sphere that could

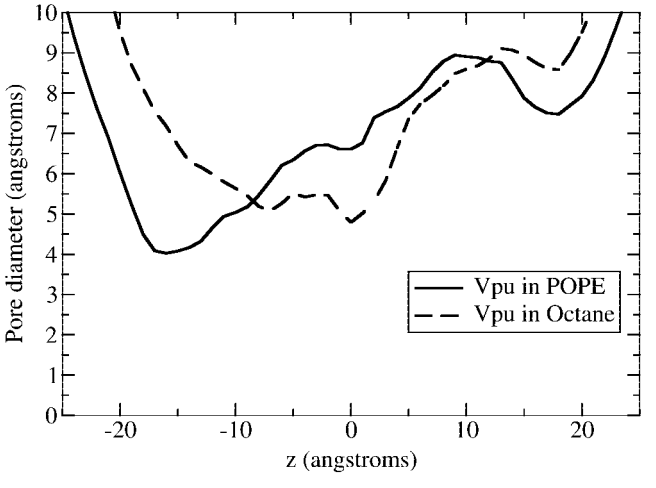

FIGURE 8 Time-averaged pore diameter along the center of the center of the VPU bundle. Some differences exist between the VPU$^{1-27}$ (*solid line*) and VPU$^{6-27}$ (*dashed line*) profiles in addition to the obvious distance mismatch. The C-terminus is on the left side (toward −20 Å) and the N-terminus is on the right side (toward +20 Å).

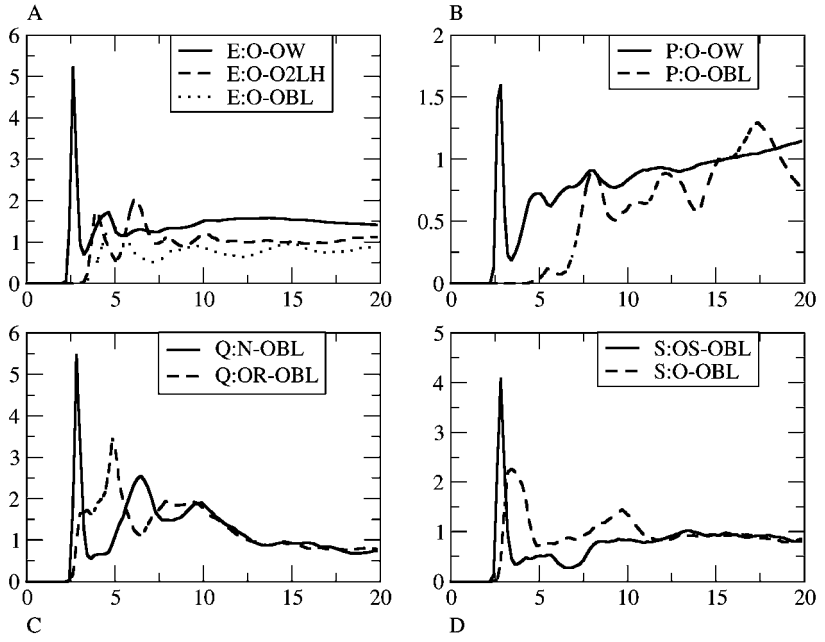

FIGURE 9 Radial distribution functions (RDF) for The E (*a*), P (*b*), Q (*c*), and S (*d*) residues are shown along with their interactions with different atoms. The atom names correspond to carboxylic oxygen in the peptide bond (O) water oxygen (OW), chain nitrogen for Q (NH2), chain oxygen for Glu (OR), and chain oxygen for S (OS). Remaining atoms named as shown in Fig. 1.

be accommodated by the bundle in the specified *x-y* plane along the pore, funnels from the N-terminus to the middle of the lipid bilayer (from +20 to zero). The differences between the two bundles, besides their obvious length disparity, lie in the narrow ("filter") region. In octane this "filter" is less pronounced, but over a 10 Å distance (0 to −10), while in the lipid case the "filter" is sharper (−12 to −18) and closely associated with the W(24) residue. The difference in the pore lengths reflects the shorter peptide distance of the VPU^{6-27} as compared to VPU^{1-27}. In addition, the hydrophobic and hydrophilic interactions of the headgroup with the residues in VPU^{1-27} will affect the dynamics of the terminal amino-acids as compared to those in VPU^{6-27}, which are in contact with water. The pore radius for both VPU-TM monomers is comparable for the −10 to 20 Å region and both pores exhibit a similar trend in their size profiles. The narrow region of the VPU^{6-27} pore is less sharp than that of the VPU^{1-27}, which again could be a direct consequence of the choice of hydrophobic medium for VPU^{6-27}.

At the ends of the pore, an increase in pore size is seen in the octane/water VPU^{6-27} system compared to that of the VPU^{1-27} bundle in POPE. On the one hand, the VPU^{1-27}-TM bundle in POPE is narrower at the ends than the bundle in octane. This makes qualitative sense because the octane/water interface lies slightly below the ends of the VPU^{6-27} bundle, allowing some residues to interact with the water directly. On the other hand, these same residues can interact with the POPE headgroups and the lateral pressure of the explicit membrane will force these to remain narrower, an effect that could contribute to the function of the channel. This agrees well with findings seen in gramicidin, where the match/mismatch of the hydrophobic and hydrophilic regions of the peptides are important for structure and function of the ion channel (Lundbaek and Andersen, 1999). Again, no shearing in the long axis of the helices was observed in this simulation.

Perhaps the most interesting finding from our simulation concerns the interactions of the helix with the lipid bilayer. In an attempt to understand the interactions between the lipid and the bundle we plot atom pair RDFs representative of the lipid and helix interactions as shown in Fig. 9. Although we have investigated all of the different amino acid residues, the RDFs we show are those that have the highest probability of interacting at close distances with the lipid molecules, namely E(2), P(3), and Q(5) on the N-terminus side and S(23) on the C-terminus side. These residues interact with the carboxyl oxygens near the glycerol in the tails of the lipid molecules and/or with the solvent molecules.

The following discussion refers to the RDFs plotted in Fig. 9. Residues 1–4 can all be in contact with the solvent and interact with water and the lipid headgroups to varying degrees. The E residue (Fig. 9 *a*) has a well-defined peak for its interaction from the carboxyl oxygen (O) and the water oxygen (OW), while it has a less well-defined interaction from the same atom with the lipid oxygen atoms. The same is true for P (Fig. 9 *b*), which has a well-defined interaction with the solvent from its carboxyl oxygen (O), but much less defined interactions with the lipid oxygen atoms. The Q residue (Fig. 9 *c*) has the strongest interaction with the lipid of the first five residues of VPU showing defined peaks for both the interactions from its side-chain nitrogen (N) and its side-chain oxygen (OR) with the lipid oxygen atoms (OBL). On the other side of the bilayer near the C-terminus most residues interact quite poorly with the lipid bilayer or water, except for the S residue (Fig. 9 *d*). Both the side-chain

oxygen (OS) and the peptide carboxyl oxygen (O) have defined interactions with the lipid oxygen atoms. The interactions of Q and S with the lipid tail carboxyl oxygen atoms suggest that there is a preferential configuration by which the bilayer "clamps" the ion channel at a certain distance. This is similar to previous finding in the gramicidin channel (Lundbaek and Andersen, 1999).

The interactions that have been established from the above analysis suggest two things. First, we can infer that there is a preferential position for the helices along the pore based on the interactions of the hydrophilic residues and the lipid charged atoms. The second shows that the interaction of hydrophobic groups with the lipid, the dynamics of W, and interactions around the carboxyl oxygen of the lipids suggest that these interactions will play an important role in the mechanism of the ion channel pore. We anticipate that most water-accessible residues are those toward the N-terminus from the W group. The occlusion of the pore by the W residues corresponds to a channel in a closed conformation. Further simulations with the inclusion of a potential across the membrane (as in the ion channel experiments) may yield insights into the open state of the channel.

CONCLUSIONS

We have reported the results of two MD simulations. The first consisted of a VPU^{6-27} hexamer bundle embedded in a membrane mimetic octane/water system. This simulation was performed both as an extension of our previous work with the pentamer and as a preliminary study for the setup of VPU^{1-27} in an explicit lipid bilayer. We conclude that VPU-TM tends to oligomerize as a pentamer under the present simulation conditions, which we postulate are representative of the accessible states of the protein.

We have also shown the results of a 3-ns MD simulation of a pentamer of VPU^{1-27} embedded in a fully hydrated POPE lipid bilayer. The MD simulation, which began with a pore of water, exhibits a closing of the pore after ~1.5 ns. We find that the interaction of the Q(5) and S(23) residues with the lipid carboxyl oxygen groups is an important factor in the observed structure of the bundle. The pentamer is essentially anchored to the bilayer by these two residues. From the radial distribution functions and electron density profile we also see that the N-terminus of the pentamer is more solvated than the C-terminus, which possibly contributes to the closed state, although interactions of the C-terminus with water are abundant. Further simulation studies will need to include longer segments of VPU, which have shown ion channel conductance activity and/or have been observed to align in NMR studies (Marassi *et al.*, 1999; Schubert *et al.*, 1996b). Previous studies on peptide bundles suggest that it might be necessary to include a potential across the membrane to help rationalize the observed ion channel behavior (Moore *et al.*, 1998).

The authors thank Dave Jones and Songyang Zheng for their input and discussions, which contributed significantly to this research project. The authors also thank Jeffrey D. Evanseck for his help with the initial setup of the VPU monomer.

This research was supported by the National Institute of Health (NIGMS) under Program Grant P01 GM56538, the Pittsburgh Supercomputing Center (PSC), and NCSA under the NPACI program.

REFERENCES

Brooks, B. R., R. E. Bruccoleri, B. D. Olafson, D. J. States, S. Swaminathan, and M. Karplus. 1983. CHARMM: a program for macromolecular energy, minimization and dynamics calculations. *J. Comp. Chem.* 4:187–217.

Feller, S. E., R. W. Pastor, A. Rojnuckarin, S. Bogusz, and B. R. Brooks. 1996. Effect of electrostatic force truncation on interfacial and transport properties of water. *J. Phys. Chem.* 100:17011–17020.

Feller, S. E., D. X. Yin, R. W. Pastor, and A. D. Mackerell. 1997. Molecular dynamics simulation of unsaturated lipid bilayers at low hydration: parameterization and comparison with diffraction studies. *Biophys. J.* 73:2269–2279.

Frankel, A. D., and J. A. T. Young. 1998. HIV-1: fifteen proteins and an RNA. *Annu. Rev. Biochem.* 67:1–25.

Gennis, R. B. 1989. Biomembranes: Molecular Structure and Function. Springer-Verlag; New York.

Grice, A. L., I. D. Kerr, and M. S. P. Sansom. 1997. Ion channels formed by HIV-1 Vpu: a modelling and simulation study. *FEBS Lett.* 405: 299–304.

Jorgensen, W. L., J. Chandrasekhar, J. D. Madura, R. W. Impey, and M. L. Klein. 1983. Comparison of simple potential functions for simulating liquid water. *J. Chem. Phys.* 92:926–935.

Kukol, A., and I. T. Arkin. 1999. VPU transmembrane peptide structure obtained by site-specific Fourier transform infrared dichroism and global molecular dynamics Searching. *Biophys. J.* 77:1594–1601.

Lamb, R., and L. H. Pinto. 1997. Do Vpu and Vpr of human immunodeficiency virus type 1 and NB of influenza B virus have ion channel activities in the viral life cycles? *Virology.* 229:1–11.

Lundbaek, J. A., and O. S. Andersen. 1999. Spring constants for channel-induced lipid bilayer deformation estimates using gramicidin channels. *Biophys. J.* 76:889–895.

Mackerell, A. D., D. Bashford, M. Bellott, R. L. Dunbrack, J. D. Evanseck, M. J. Field, S. Fischer, J. Gao, H. Guo, S. Ha, J. D. McCarthy, L. Kichnir, K. Kuczera, F. T. K. Lau, C. Mattos, S. Michnick, T. Ngo, D. T. Nguyen, B. Prodhom, W. E. Reiher, B. Roux, M. Schlenkrich, J. C. Smith, R. Stote, J. Straub, M. Watanabe, J. Wiorkiewicz-Kuczera, D. Yin, and M. Karplus. 1998. All-atom empirical potential for molecular modeling and dynamics studies of proteins. *J. Phys. Chem. B.* 102: 3586–3616.

Marassi, F. M., C. Ma, H. Gratkowski, S. K. Straus, K. Strebel, M. Oblatt-Montal, M. Montal, and S. J. Opella. 1999. Correlation of the structural and functional domains in the membrane protein Vpu from HIV-1. *Proc. Natl. Acad. Sci. USA.* 96:14336–14341.

Marassi, F. M., and S. J. Opella. 2000. A solid-state NMR index of helical membrane protein structure and topology. *J. Magn. Reson.* 144: 150–155.

Moore, P. B., and M. L. Klein. 1997. Implementation of a General Integration for Extended System Molecular Dynamics. Tech. Rep., University of Pennsylvania. http://www.cmm.upenn.edu/moore/code/code.html.

Moore, P. B., C. F. Lopez, and M. L. Klein. 2001. Structure and dynamics of water on a hydrated DMPC lipid bilayer at the interface from a molecular dynamics simulation. *Biophys. J.* 5:2484–2494.

Moore, P. B., Q. Zhong, T. Husslein, and M. L. Klein. 1998. Simulation of the HIV-1 Vpu transmembrane domain as a pentameric bundle. *FEBS Lett.* 431:143–148.

Norberg, J., and L. Nelsson. 2000. On the truncation of long-range electrostatic interactions in DNA. *Biophys. J.* 79:1537–1553.

Sansom, M. S. P., L. R. Forrest, and R. Bull. 1998. Viral ion channels: molecular modeling and simulation. *Bioessays.* 20:992–1000.

Schubert, U., S. Bour, A. V. Ferrer-Montiel, M. Montal, F. Maldarelli, and K. Strebel. 1996a. The two biological activities of human immunodeficiency virus type 1 Vpu protein involve two separable structural domains. *J. Virol.* 70:809–819.

Schubert, U., A. V. Ferrer-Montiel, M. Oblatt-Montal, P. Henklein, K. Strebel, and M. Montal. 1996b. Identification of an ion channel activity of the Vpu transmembrane domain and its involvement in the regulation of virus release from HIV-1-infected cells. *FEBS Lett.* 398:12–18.

Siepmann, J. I., S. Karaborni, and B. Smit. 1993. Simulating the critical behavior of complex fluids. *Nature.* 365:330–332.

Tiganos, E., J. Friborg, B. Allain, N. G. Daniel, X. Yao, and E. A. Cohen. 1998. Structural and functional analysis of the membrane spanning domain of the human immunodeficiency virus type 1 Vpu protein. *Virology.* 251:96–107.

Tuckerman, M. J., B. J. Berne, and G. J. Martyna. 1992. Reversible multiple time scale molecular dynamics. *J. Chem. Phys.* 97:1990–2001.

Tuckerman, M. E., and G. J. Martyna. 2000. Understanding modern molecular dynamics: techniques and applications. *J. Phys. Chem. B.* 104:159–178.

Turner, B. G., and M. F. Summers. 1999. Structural biology of HIV. *J. Mol. Biol.* 285:1–32.

Willbold, D., S. Hoffmann, and P. Rosch. 1997. Secondary structure and tertiary fold of the human immunodeficiency virus protein U (Vpu) cytoplasmic domain in solution. *Eur. J. Biochem.* 245:581–588.

Zheng, S. Y., J. Strzalka, C. Ma, S. J. Opella, B. M. Ocko, and J. K. Blasie. 2001. Structural studies of the HIV-1 accessory protein Vpu in Langmuir monolayers: x-ray reflectivity. *Biophys. J.* 80:1837–1850.